1    **Measurement report: Chemical characteristics of PM$_{2.5}$ during typical biomass**

2    **burning season at an agricultural site of the North China Plain**

3    Linlin Liang[1], Guenter Engling[2,3], Chang Liu[1], Wanyun Xu[1], Xuyan Liu[4], Yuan Cheng[5], Zhenyu

4    Du[6], Gen Zhang[1], Junying Sun[1], Xiaoye Zhang[1]

5    [1] State Key Laboratory of Severe Weather & Key Laboratory for Atmospheric Chemistry, Chinese

6    Academy of Meteorological Sciences, Beijing 100081, China

7    [2] Division of Atmospheric Sciences, Desert Research Institute, Reno, NV 89512, USA

8    [3] Now at: California Air Resources Board, El Monte, CA 91731, USA

9    [4] National Satellite Meteorological Center, Beijing 100081, China

10    [5] School of Environment, Harbin Institute of Technology, Harbin 150001, China

11    [6] National Research Center for Environmental Analysis and Measurement, Beijing 100029 China

12    **Abstract:**

13    Biomass burning activities are ubiquitous in China, especially in North China, where there is an

14    enormous rural population and winter heating custom. Biomass burning tracers (i.e., levoglucosan,

15    mannosan  (MN) and potassium (K$^+$)), as well as other chemical components were quantified at a

16    rural site (Gucheng, GC) in North China from 15 October to 30 November, during a transition

17    heating season, when the field burning of agricultural residues was becoming intense. The measured

18    daily average concentrations of ~~LG~~levoglucosan, mannosan~~MN~~ and K$^+$ in PM$_{2.5}$ during this study

19    were 0.79 ± 0.75 μg m$^{-3}$, 0.03 ± 0.03 μg m$^{-3}$ and 1.52 ± 0.62 μg m$^{-3}$, respectively. Carbonaceous

20    components and biomass burning tracers showed higher levels at nighttime than daytime, while

21    secondary inorganic ions were enhanced during daytime. An episode with high levels of biomass

22    burning tracers was encountered at the end of October, 2016, with high ~~LG~~levoglucosan at 4.37 μg

23    m$^{-3}$. Based on the comparison of chemical components during different biomass burning pollution

24    periods, it appeared that biomass combustion can obviously elevate carbonaceous components

25    levels, whereas no essentially effect on secondary inorganic aerosols in the ambient air. Moreover,

26    the levoglucosan~~LG~~/mannosan~~MN~~ ratios during different biomass burning pollution periods

27    remained at high values (in the range of 18.3 - 24.9), however, the levoglucosan~~LG~~/K$^+$ ratio was

28    significantly elevated during the intensive biomass burning pollution period (1.67) when air

29  temperatures decreasing, substantially higher than in other biomass burning periods (averaged at

30  0.47).

31  *Keywords*: Biomass burning; Organic tracers; Levoglucosan; Mannosan; Potassium

## 1. Introduction

33      Particulate air pollution is attracting more and more concerns in China because of their obvious

34  adverse impact on visibility reduction, as well as health implication and regional or global climate

35  change (Kanakidou et al., 2009; Pope and Dockery, 2006; Cheng et al., 2016). Carbonaceous species,

36  i.e., organic carbon (OC) and elemental carbon (EC), and water-soluble inorganic ions, e.g., $SO_4^{2-}$,

37  $NO_3^-$ and $NH_4^+$ are the major components of ambient aerosols (Liang et al., 2017; Du et al., 2014;

38  Zheng et al., 2015; Tan et al., 2016). Biomass burning (BB) emissions constitute a large source of

39  ambient particulate pollution, especially for carbonaceous components, i.e., primary organic carbon

40  (POC) and black carbon (BC) on global scale (Bond et al., 2004; Tang et al., 2018; Titos et al., 2017).

41  As an important aerosol component, black carbon from industrial and combustion emissions

42  contributes to the enhanced $PM_{2.5}$ (particulate matter with aerodynamic diameters less than 2.5 µm)

43  mass concentrations and influences regional radiative forcing (Chen et al., 2017). Fresh biomass

44  burning aerosol was found to be mainly comprised of carbonaceous species which typically

45  constitutes 50-60% of the total particle mass (Hallquist et al., 2009). Yao et al. (2016) identified

46  approximately half of carbonaceous aerosols being contributed by biomass burning at Yucheng, a

47  rural site in the North China Plain.

48      Biomass burning emissions also represent a potentially large source of secondary organic

49  aerosol (SOA). The precursors and formation pathways of SOA from biomass burning emissions

50  were investigated by extensive field observations (e.g., Zhu et al., 2015; 2017; Adler et al., 2011;

51  Zhang et al., 2010; 2015). Based on morphological particle analysis, Yao et al. (2016) investigated

52  the smoke emitted from biomass burning impacting SOA production. Sun et al. (2010) found that

53  phenolic compounds, which were emitted in large amounts from wood combustion, can form SOA

54  at high yields in aqueous-phase reactions. In addition, smoke from biomass burning can be

55  transported thousands of kilometers downwind from the source areas. Biomass burning aerosol from

56  Southeast Asia can be transported to China, Singapore and even further to North America (Liang et

al., 2017; Hertwig et al., 2015; Peltier et al., 2008). Based on molecular tracer measurements, synoptic data as well as air mass back trajectory analysis, a fire episode was captured at a background site of East China with smoke advected from Southeast Asia (Liang et al., 2017).

The North China Plain (NCP) is one of the most polluted regions in China. Severe haze–fog of longer duration and more extensive coverage has occurred frequently in the NCP area, especially during the seasons of autumn and winter. NCP covers one quarter of China's cultivated land and yields 35% of the agricultural products in China (Boreddy et al., 2017). The rural population in NCP is also large and dense, and biomass burning activities are common in this region in form of cooking and heating. Intense fire activity typically occurs in October after the corn harvest. Abundant smoke is emitted from agricultural burning, i.e., residential biofuel combustion, open field burns, etc. Various field observations have investigated different aspects of biomass burning, e.g., seasonal variations, chemical and physical properties of smoke particles, spatial distribution, sources, transport, etc., in the NCP region (Cheng et al., 2013; Shen et al., 2018; Sun et al., 2013; 2016; Boreddy et al., 2017; Xu et al., 2019). However, these field investigations of the contribution of biomass burning to ambient aerosols in the NCP region were concentrated on the city of Beijing (Cheng et al., 2013; Zheng et al., 2015; Duan et al., 2004). Little field research about biomass burning was reported for rural areas in the NCP. In fact, biomass burning activities are common in the rural areas of the NCP region, and the resulting smoke aerosol can be transported to urban areas, e.g., the city of Beijing, resulting in haze episodic events.

~~The objective of this study is gain insights about the abundance of smoke during the typical biomass burning season, i.e., autumn-winter transition season, following the corn harvest. In this paper, we focus on quantifying multiple biomass burning tracers, i.e., levoglucosan~~LG, ~~mannosan~~MN and K$^+$ ~~as well as other chemical species in PM$_{2.5}$ in the rural areas of the NCP region during the typical biomass burning season.~~ In order to characterize the biomass burning pollution status within rural areas of the NCP region, multiple biomass burning tracers, i.e., levoglucosan, mannosan and K$^+$ in PM$_{2.5}$ sampled at a heavily polluted rural site in Hebei province were quantified during a typical biomass burning season, i.e., autumn-winter transition season, following the corn harvest. Combined with the analysis of other chemical components, it reveals different levels of biomass combustion pollution impacting on different types of chemical components in ambient

aerosol. Meanwhile, based on the multi-analysis of biomass burning molecular tracers, back trajectory analysis, fire activity data and synoptic conditions, the results of this study demonstrate the biomass burning pollution status, as well as the formation process of severe biomass burning pollution episode in the rural atmosphere of North China. These results can provide valuable information about the biomass burning activities in all of Northern China.

~~The results of this study demonstrated the biomass burning pollution status, as well as chemical properties of ambient aerosols under different biomass burning pollution levels in the rural atmosphere of North China.~~

## 2. Site description and experimental Methods

### 2.1 Site description and sampling

Samples were collected at a rural site, Gucheng (GC, 39°09'N, 115°44'E; 15.2 m a.s.l), located on a platform at the China Meteorological Administration farm in the town of Gucheng (GC site), approximately 110 km southwest of Beijing and 35 km north of the city of Baoding (population of about 5 million) in Hebei province, as shown in Figure S1. The station is surrounded by agricultural fields, with major crop species being corn and wheat. The dominant wind direction at GC is southwest and northeast during the study period. This site is upwind of Beijing, when the wind blows from the south or southwest, where heavily polluted cities and regions of Hebei province, i.e., Baoding, Shijiazhuang, Xingtai, Handan, are located. Thus, it is an appropriate station for representing the air pollution situation in the NCP region (Sheng et al., 2018; Chi et al., 2018; Xu et al., 2019; 2020; Kuang et al., 2020).

Daytime and nighttime $PM_{2.5}$ samples were collected from 15 October, 2016 to 23 November, 2016, by using $PM_{2.5}$ High-volume (Hi-Vol) sampler (GUV-15HBL1, Thermo Fisher Scientific CO., LTD), at the nominal flow rate of 1.13 $m^3$ $min^{-1}$. The daytime samples were collected from 07:00 to 19:00, while nighttime samples were collected from 19:00 to 07:00 local time of the next day. All $PM_{2.5}$ samples were collected on quartz fiber filters, prebaked at 850 °C for at least 5 h to remove carbonaceous material. A total of 33 couples of daytime/nighttime samples and 6 whole-day samples as well as 4 field blank samples were collected during the sampling period. The filters were stored at -20 °C after sample collection.

**2.2 Experimental Methods**

**2.2.1 Anhydrosugar and water-soluble inorganic ion analysis**

The quartz filter samples were analyzed for biomass burning anhydrosugar tracers, i.e., levoglucosan and mannosanLG and MN, using an improved high-performance anion-exchange chromatography (HPAEC) method with pulsed amperometric detection (PAD) on a Dionex ICS-5000+ system. LevoglucosanLG and mannosanMN were separated by a Dionex Carbopac MA1 analytical column and guard column with an aqueous sodium hydroxide (NaOH, 480 mM) eluent at a flow rate of 0.4 mL min$^{-1}$. The detection limit of levoglucosanLG and mannosanMN was 0.002 mg L$^{-1}$ and 0.005 mg L$^{-1}$, respectively. More details about the HPAEC-PAD method can be found elsewhere (Iinuma et al., 2009).

The quartz filter samples were also analyzed for water-soluble inorganic ions by a Dionex ICS-5000+ ion chromatograph, including $SO_4^{2-}$, $NO_3^-$, $NH_4^+$, $Cl^-$, $Ca^{2+}$, $Na^+$, $K^+$ and $Mg^{2+}$, and the method detection limits for the individual ionic species were 0.18 µg L$^{-1}$, 0.15 µg L$^{-1}$, 0.03 µg L$^{-1}$, 0.048 µg L$^{-1}$, 0.08 µg L$^{-1}$, 0.01 µg L$^{-1}$, 0.01 µg L$^{-1}$, 0.008 µg L$^{-1}$, respectively. The cations were separated on an Ionpac CS12 analytical column and CG12 guard column with a 20 mM methanesulfouic acid as eluent at a flow rate of 1.0 mL min$^{-1}$, while the anions were separated on an Ionpac AS11-HC column and AG11-HC guard column with 21.5 mM KOH eluent at a flow rate of 1.0 mL min$^{-1}$. The water-soluble inorganic ion data were corrected by field blanks.

**2.2.2 Organic carbon/elemental carbon analysis**

OC and EC were measured on a punch (0.526 cm$^2$) of each quartz sample by a thermal/optical carbon analyzer (DRI Model 2001, Desert Research Institute, USA), using the Interagency Monitoring of Protected Visual Environments (IMPROVE) thermal evolution protocol with reflectance charring correction. The analytical error of OC was within 10%, and one sample of every 10 samples was selected at random for duplicate analysis. The detection limit of OC was 0.82 µgC cm$^{-2}$ (Liang et al., 2017).

**2.2.3 Gas online monitoring (i.e., NO, NO$_2$, SO$_2$, O$_3$, CO and NH$_3$)**

During this campaign, commercial instruments from Thermo Fisher Scientific Co., LTD were used to measure O$_3$ (TE 49C), NO/NO$_2$/Nox (Model 42CTL), CO (TE 48CTL), and SO$_2$ (TE43CTL), while NH$_3$ was measured by an ammonia analyzer (DLT-100, Los Gatos Research,

143  USA) at GC station. All measurement data quality was controlled according to standard gases (Xu

144  et al., 2019; Lin et al., 2011; Meng et al., 2018; Ge et al., 2018).

145  **2.2.4 Meteorological parameters**

146  The meteorological parameters, including air temperature, relative humidity (RH) and wind

147  speed at a 24-h resolution at the GC site are presented in Figure 1. During this campaign, the daily

148  average RH value was observed at $77 \pm 13\%$, with a range from 48% to 99%, while the daily wind

149  speed was observed with an average value of $1.07 \pm 1.14$ m s$^{-1}$, exhibiting moist and stable synoptic

150  conditions at this rural site during the autumn-winter transition season. Moreover, there was rare

151  precipitation during the sampling period at the GC site, except for two days, i.e., 20 and 27 October,

152  2016 (Figure 1).

153  **2.2.5 Back trajectory and fire spot analysis**

154  To characterize the transport pathways of the aerosol at the Gucheng site, back-trajectories

155  were calculated with the NOAA Hybrid Single-Particle Lagrangian Integrated Trajectory

156  (HYSPLIT) model via NOAA ARL READY Website (http://ready.arl.noaa.gov/HYSPLIT.php).

157  To investigate the influence of biomass burning activities in surrounding areas, fire hot spot

158  counts were obtained from the Fire Information for Resource Management System (FIRMS)

159  (available at https://firms.modaps.eosdis.nasa.gov/download/).

160  **2.2.6 –Statistical analysis**

161  Statistical analysis of data, i.e., the correlation analysis between the concentrations of

162  levoglucosan, mannosan and K$^\pm$ at the Gucheng site during the sampling period were conducted

163  with the linear fitting method.

164

165  **3. Results and discussion**

166  **3.1 Characteristics of chemical components in PM$_{2.5}$**

167  In this study, the mass concentration of PM$_{2.5\text{-cal}}$ was reconstituted by the sum of carbonaceous

168  components ($1.6 \times OC + EC$) and inorganic ions ($SO_4^{2-} + NH_4^+ + NO_3^- + Cl^- + Ca^{2+} + Na^+ + K^+ +$

169  $Mg^{2+}$). Figure 1 describes the time-series variation obtained for daily PM$_{2.5\text{-cal}}$, and its major

170  components (OC, EC, $SO_4^{2-}$, $NO_3^-$ and $NH_4^+$), biomass burning tracers (levoglucosanLG,

171    mannosan~~MN~~ and K$^+$), ratios of levoglucosan/OC and meteorological factors (temperature ~~(T)~~,

172    ~~relative humidity (~~RH~~)~~, wind speed ~~(WS)~~ and planetary boundary layer (PBL) height ~~rainfall~~)

173    during the sampling period. The average daily PM$_{2.5\text{-cal}}$ mass concentration in the autumn-winter

174    transition season at GC reached $137 \pm 72.4$ µg m$^{-3}$, ranging from 23.3 µg m$^{-3}$ to 319 µg m$^{-3}$ (Table

175    1, Figure 1a), which is higher than during the severe winter haze in January, 2013 at an urban site

176    in Beijing (121 µg m$^{-3}$) (Zheng et al., 2015). The mass concentrations of these chemical species

177    during the day are distributed as follows (from highest to lowest): $OC > EC > NO_3^- > SO_4^{2-} >$

178    $NH_4^+ > Cl^- > Ca^{2+} > K^+ > Na^+ > Mg^{2+}$. Organic matter (OM), calculated by multiplying OC values

179    with a coefficient of 1.6, was the most abundant PM component, the daily average value of which

180    was $70.4 \pm 49.6$ µg m$^{-3}$, accounting for nearly half (46.7%) of PM$_{2.5\text{-cal}}$ mass, indicating obvious

181    organic pollution at the rural site in the North China Plain during the sampling season.

182        The measured daily average concentrations of biomass burning tracers, i.e., levoglucosan ~~LG~~,

183    mannosan~~MN~~ and K$^+$ in PM$_{2.5}$ during our study were $0.79 \pm 0.75$ µg m$^{-3}$, $0.03 \pm 0.03$ µg m$^{-3}$ and

184    $1.52 \pm 0.62$ µg m$^{-3}$, respectively (Table 1). The ~~anhydrosugar~~ ambient concentrations of

185    levoglucosan ~~levels (levoglucosanLG and mannosanMN)~~ in this study were higher than those

186    observed in the city of Beijing during the summer (averaged at $0.23 \pm 0.37$ µg m$^{-3}$, in the range of

187    0.06 to 2.30 µg m$^{-3}$) and winter (averaged at $0.59 \pm 0.42$ µg m$^{-3}$, in the range of 0.06 to 1.94 µg m$^{-3}$

188    ) of 2010-2011 (Cheng et al., 2013). The biomass burning tracer levels and ratios observed in this

189    study and other field studies are summarized in Table S1. The highest concentrations of

190    levoglucosan ~~LG~~ in GC were observed on 31 October, 2016 with 4.37 µg m$^{-3}$, which is a sharp

191    increase (over 30 times) of the minimum concentration (0.14 µg m$^{-3}$) during that period (Figure 1c).

192    Accordingly, the PM$_{2.5\text{-cal}}$ concentration during that period was also elevated (as high as 236 µg m$^{-3}$

193    ) (Figure 1a). Secondary inorganic aerosol (sulfate, $SO_4^{2-}$; nitrate, $NO_3^-$ and ammonium, $NH_4^+$,

194    SNA) species, were the major water soluble ions, accounting for 82.8% of total water soluble ions,

195    the daily average values of which were $10.5 \pm 6.87$ µg m$^{-3}$, $15.9 \pm 9.29$ µg m$^{-3}$ and $10.9 \pm 5.51$ µg

196    m$^{-3}$, respectively (Table 1). SNA species exhibited a synchronous temporal trend (Figure 1c), while

197    the $NO_3^-$ concentrations exceeded those of $SO_4^{2-}$ at the GC site, in contrast to the results of previous

198    studies, e.g., Tan et al. (2016), who found $SO_4^{2-}$ to be the dominant species in PM$_{2.5}$ during winter

199    in 2006 in Beijing. Similarly, Chi et al., (2018) also found $NO_3^-$ concentrations exceeded those of

SO$_4^{2-}$ at both Beijing and GC sites during the winter in 2016, although they observed that NH$_4^+$ was the dominant component of SNA (the concentrations of SO$_4^{2-}$, NO$_3^-$ and NH$_4^+$ were 14.0 μg m$^{-3}$, 14.2 μg m$^{-3}$, and 24.2 μg m$^{-3}$, respectively).

**3.2 Day-night variations in the characteristics of PM$_{2.5}$ chemical components**

Carbonaceous components and biomass burning tracers exhibited higher levels during nighttime than daytime, while secondary inorganic ions showed the opposite pattern, i.e., higher concentrations during daytime than nighttime (Figure 2 and Figure S2). Besides, the gap of carbonaceous components and anhydrosugars between daytime and nighttime (two-fold) was more significant than for secondary inorganic ions. EC and ~~primary organic components~~POC are not subject to significant differences in chemical reactions in ambient air between daytime and nighttime, and they will be mainly influenced by the variations of the ~~planetary boundary layer~~ (PBL~~)~~ height. In the night, the PBL height decreases, compressing air pollutants into a shallow layer, and subsequently resulting in faster accumulation and higher concentrations of pollutants (Zheng et al., 2015; Zhong et al., 2018; 2019). The contributions of OM and EC to PM$_{2.5\text{-cal}}$ were observed to be higher at nighttime (53.9% and 16.6%) than daytime (43.8% and 13.7%) as well (Figure 3).

Besides the influence from variations of the PBL height, the chemical degradation of levoglucosan may occur due to photochemical reaction in the ambient aerosols during day-time, further enlarging the gap of levoglucosan levels ~~in~~ between daytime and nighttime (Sang et al., 2016; Gensch et al., 2018). Consequently, ~~T~~the contribution of levoglucosan to PM$_{2.5\text{-cal}}$ during daytime (~~0.37~~0.45%) was observed to be considerably lower than that during nighttime (0.64%) (Figure 3). However, secondary inorganic ions have an important formation pathway, i.e., photochemical processing, during daytime. Thus, the secondary inorganic species (SO$_4^{2-}$, NO$_3^-$ and NH$_4^+$) were enhanced during daytime due to photochemical formation (Sun et al., 2013; Zheng et al., 2015; Wu et al., 2018). The mass contributions of SO$_4^{2-}$, NO$_3^-$ and NH$_4^+$ to PM$_{2.5\text{-cal}}$ were decreased from daytime (9.9%, 14.5% and 10.0%) to nighttime (6.5%, 9.6% and 7.1%) (Figure 3). Such an enhancement in secondary transformations during daytime is more evident in terms of the sulfur and nitrogen oxidation ratios (SOR and NOR, molar ratio of sulfate or nitrate to the sum of sulfate and SO$_2$ or nitrate and NO$_2$), which have been used previously as indicators of secondary transformations (Sun et al., 2013; Zheng et al., 2015). Both SOR and NOR during daytime were

higher than those during nighttime (Figure S3), further confirming the elevated secondary formations of sulfate and nitrate during daytime.

In addition, the concentrations of other water-soluble inorganic ions, i.e., $K^+$ and $Cl^-$ during nighttime ($1.78 \pm 0.95$ µg m$^{-3}$ and $6.08 \pm 4.00$ µg m$^{-3}$) were higher than those in daytime ($1.43 \pm 0.54$ µg m$^{-3}$ and $4.33 \pm 2.30$ µg m$^{-3}$), while their contributions to PM$_{2.5-cal}$ were reversed, due to the significant accumulation and higher concentrations of pollutants during nighttime. As $Ca^{2+}$, $Mg^{2+}$ and $Na^+$, mainly emitted from primary natural sources, such as dust, soil resuspension and sea salt, are subject to more activity during the daytime and also influenced by the airflow dynamics, the contribution of those species in nighttime were lower than those during daytime, especially for $Ca^{2+}$, decreasing from 2.2% in daytime to 0.9% at nighttime (Figure 3).

**3.3 Biomass burning episodes and the impacts on chemical PM$_{2.5}$ characteristics**

An episode with high biomass burning tracer levels was encountered on 31 October, 2016. The concentrations of levoglucosan~~LG~~ in PM$_{2.5}$ during this one-day episode (4.37 µg m$^{-3}$) were significantly higher than those during typical transition season at the GC site ($0.69 \pm 0.47$ µg m$^{-3}$) (Figure 1d). Meanwhile, there was significant change in the meteorological conditions, i.e., the wind direction changed from southwesterly to northerly winds (Figure S4). Northerly winds advected cold and dry air masses, with the lowest hourly temperature observed at -5.3 °C (Figure S5). This notable temperature decline before the commencing of the operation of the central heating systems should have caused intense combustion activities for heating purposes at the rural site. Moreover, the synoptic situation on 31 October, 2016 was under weaker turbulence with low PBL height and small wind speeds (Figure 1f). These worsened meteorological conditions would further enhance aerosol accumulation.

Here, we mainly distinguish four sub-periods based on daily ~~—~~levoglucosan~~LG~~ concentrations during the time frame from 15 October to 23 November, 2016. The four periods were separated as follows: 15-30 October (Period I: Minor biomass burning), 31 October (Period II: Intensive biomass burning), 1-14 November (Period III: Major biomass burning), 15-23 November (Period IV: Heating season). Table 2 compares the concentrations of PM$_{2.5-cal}$ mass, chemical components and gases at the GC site during these four periods, as well as the ratios between the intensive, major BB periods and heating season to minor BB period. The level of levoglucosan ~~LG~~

during the intensive BB episode II was about 12 times of that during the minor BB period I. $K^+$ and

$Cl^-$, the common biomass burning tracers utilized in many studies (Duan et al., 2004; Cheng et al.,

2013), were also observed with increased abundance during intensive BB episode II. When entering

into November, the weather was becoming cold, and thus combustion activities for heating in the

rural areas commenced, resulting in the ambient levels of levoglucosan~~LG~~ to increase to $0.92 \pm 0.47$

$\mu g \ m^{-3}$ during period III, about 3 times of those in Period I. The central heating systems in North

China cities were operated during period IV, and the ambient level of levoglucosan~~LG~~ was observed

at $0.96 \pm 0.63 \ \mu g \ m^{-3}$, which was similar to that observed in period III.

The concentrations of OC and EC were also observed to be strongly elevated in period II (Table

2), and especially OC levels increased to ~~59.9~~96.3 ~~± 25.3~~ $\mu g \ m^{-3}$ during the intensive BB episode II,

nearly 6 times of ~~that~~ those during the minor BB period ($16.2 \pm 7.52 \ \mu g \ m^{-3}$). The levoglucosan/OC

ratio was utilized to estimate the effect of biomass burning to ambient organic aerosols. Accordingly,

levoglucosan~~LG~~/OC ratios sharply increased to 0.045 during period II, which ~~is~~ was

~~obvious~~noticeably higher than during other periods in this study (Figure 1e). Moreover, this level is

also higher than most of the published field observations, i.e., at urban sites (Zhang et al., 2008;

Cheng et al., 2013; Zhang et al., 2014), rural sites (Sang et al., 2013; Ho et al., 2014; Pietrogrande

et al., 2015; Mkoma et al., 2013) and agricultural sites (Ho et al., 2014; Jung et al., 2014), yet lower

than at an urban site in northern Italy during winter time (in the range of 0.01 to 0.13) (Pietrogrande

et al., 2015). This illustrates that biomass combustion played an important role in organic aerosol

pollution during the intensive BB episode II. However, ~~During the major BB (period III) and heating~~

~~season (period IV),~~ due to other emissions of OC enhanced during the major BB episode (period III)

and heating season (period IV), i.e., combustion of coal and biofuel for heating, OC increased to a

higher level ($55.2 \pm 17.1 \ \mu gC \ m^{-3}$ and $69.4 \pm 24.6 \ \mu gC \ m^{-3}$, respectively). Due to the abundance of

organic aerosols, the contribution from biomass burning emission was thereby reduced and the

levoglucosan~~LG~~/OC ratios during periods III and IV decreased to $0.016 \pm 0.005$ and $0.014 \pm 0.006$,

respectively, even lower than those observed in the minor BB period I ($0.025 \pm 0.008$).

Compared to the carbonaceous components, the concentrations of secondary inorganic aerosol

species ($SO_4^{2-}$, $NO_3^-$, $NH_4^+$) exhibited a different pattern, i.e., showing no obvious differences

between minor BB period I and other three periods. The ratios of $SO_4^{2-}$, $NO_3^-$, $NH_4^+$ during periods

II, III and IV to period I were all around 1.0 (Table 2), with no increasing trend. Moreover, the relationships between levoglucosan LG and OC (and EC) were better than those between levoglucosanLG and SNA during daytime and nighttime (Figure S3). The precursor gases of SNA, i.e., $SO_2$, $NO$, $NO_2$ and $NH_3$, were observed to have an increasing trend when biomass burning was prevalent during periods III and IV, with the ratios to period I arranged from 1.13 to 1.90 (Table 2). The time-series variations of the gases ($SO_2$, $NO_x$, $NH_3$, $CO$ and $O_3$) and PBL during the sampling period are shown in Figure S4. The primary emission gases were exhibited negative relationships with PBL, while $O_3$ exhibited obvious positive relationship with PBL (Figure S5). Combustion from different fossil fuels (coal, gasoline, diesel, etc.) and biomasses (straws, woods, leaves, etc.) can all emit CO into the atmosphere (Streets et al., 2003; Chantara et al., 2019; Merico et al., 2020). Due to the more abundant combustion in the colder weather, the concentrations of CO also increased to $1.65 \pm 0.53$ ppm and $1.18 \pm 0.83$ ppm during the major biomass burning period III and the heating season period IV, respectively.

The combustion of biomass, especially of agricultural residues (e.g., wheat and corn straw) is very common in the rural areas in North China during the autumn-winter transition period. During the autumn harvest season in North China, wheat and corn straw burning is common practice, resulting in more abundant fire spots when entering into November than period I (Figure 4). The intense biomass burning event on 31 October, 2016 was also supported by air mass back trajectory analysis (Figure 5), performed with the TrajStat software. Based on the 48 h back trajectories at the GC site at 00:00 (UTC time) on 1 November, 2016, the air mass at the GC site was restricted in the region of Bejing-Tianjing-Hebei, the polluted area where fire spots were numerous. However, on the previous and following day of this episode, i.e., 31 October and 2 November onward, the air masses arriving at GC were advected from the northwest of Mongolia, where mostly desert areas are present, with less farm land and rare biomass burning activities (Figure 5).

Mean percentiles of major components in $PM_{2.5}$ with respect to different BB pollution periods at GC site during the sampling time are shown in Figure 6. With the variation of BB pollution periods, the EC fraction seems to exhibit no obvious change during periods I, II and III, but slightly increased during the heating season (period IV), while the OC fraction increased significantly from 34.0% during the minor BB period I elevated to 65.4% during the intense BB period II. The

316  contributions of sulfate, nitrate and ammonium to $PM_{2.5-cal}$ all decreased sharply from the minor BB

317  period to the intense period (Figure 6). This suggests that organic aerosol species become more

318  important during BB pollution periods, concerning their contribution to the $PM_{2.5-cal}$, while EC has

319  no such character. The OM percentage during intense BB period II was 65.4%, about double of that

320  during the minor biomass burning period (34.0%), indicating that there was a large fraction of OM

321  in $PM_{2.5-cal}$ originating from BB at the GC site during intensive BB period II. Opposite to OM,

322  contributions of secondary inorganic ions to $PM_{2.5-cal}$ significantly decreased with the BB pollution

323  becoming more severe. The contributions of $SO_4^{2-}$, $NO_3^-$ and $NH_4^+$ to $PM_{2.5-cal}$ during the minor

324  BB episode (11.6%, 20.5% and 12.5%) obviously declined during the intense BB episode (1.~~73~~93%,

325  7.~~73~~67% and 4.24%).

## 3.4 Relationships among tracers during different biomass burning pollution periods

328  In addition to pollution level information of biomass burning molecular tracers, the ratios

329  between them could also be used to identify the different biomass types or indicate the burning

330  formation processes of atmospheric aerosols. Levoglucosan and mannosan showed a good

331  relationship during the entire sampling period (Figure 7a, $r$ = 0.97, $p$ < 0.01). The

332  levoglucosan~~LG~~/mannosan~~MN~~ ratios during minor, intense, major biomass pollution and heating

333  season periods were observed at high values, i.e., 24.9, 24.1, 24.8 and 18.3 respectively (Table 2,

334  Figure 7). ~~LG and MN in the four periods showed a good relationship (Figure 7a, R²~~ =

335  ~~0.94).~~Compared to the former three episodes (24.1 to 24.9, averaged at 24.6), the

336  levoglucosan/mannosan ration during the heating season period (18.3) decreased by 25.6%. Based

337  on source emission studies, the levoglucosan~~LG~~/mannosan~~MN~~ ratios from crop residue burning,

338  i.e., rice straw, wheat straw and corn straw, are similar and are characterized by high values

339  (averaged at 29, in the range of 12 to 55) (Zhang et al., 2007; Engling et al., 2009; Cheng et al.,

340  2013; Jung et al., 2014), yet ~~overlapped~~ overlapping with those from hardwood (averaged at 28, in

341  the range of 11 to 146) (Bari et al., 2009; Jung et al., 2014) and grass burning (18.2 ± 10.2~~>10.0~~)

342  (Sullivan et al., 2008), while softwood is characterized by relatively lower

343  levoglucosan~~LG~~/mannosan~~MN~~ ratios (averaged at 4.3, in the range of 2.5 to 4.7~~<5.0~~) (Engling et

al., 2006; Cheng et al., 2013; Jung et al., 2014). Subsequently, this declining trend ~~of~~in the levoglucosan/mannosan ratios during the heating season period was partly caused~~contributed~~ by the higher~~raised~~ proportion of softwood combustion, which is characterized by relatively lower levoglucosan/mannosan ratios. According to the local habits, soft woods, e.g. China fir and pine are also commonly used as biofuels for stove heating in North China, since they allow sustained~~long-time~~ heating duration.

The concentrations of levoglucosan~~LG~~ and $K^+$ during minor, major BB episode and heating season were correlated well (Figure 7b, $r = 0.84$, $p < 0.01$), while the red dot of period II being off from the fitted regression line. The levoglucosan~~LG~~/$K^+$ ratios during periods III and IV (~~0.52~~0.51 and 0.53) were similar to those during a BB episode at an urban site in Beijing during winter time (levoglucosan~~LG~~/$K^+$ = 0.51) (Cheng et al., 2013). However, the levoglucosan~~LG~~/$K^+$ ratio during the intense BB period II increased to 1.67, which was significantly higher than that in typical straw combustion (< 1.0). Correspondingly, there was a significant drop in temperatures at the GC site during period II, with the average daily temperature sharply decreasing from 7.5 °C on 30 Oct to 0.31 °C on 31 October, 2016, and the average temperature at night of 31 October even decreased to -3.4 °C (Figure 1g). Hence, the combustion activities were apparently intense around the sampling site for heating purposes. Compared to $K^+$, there is a large enrichment of levoglucosan~~LG~~ in wood burning emissions, based on the results from previous biomass source combustion studies (Engling et al., 2006; Chantara et al., 2019). The influence of softwood and/or other materials from softwood, which are commonly used as biofuels for stove heating in North China (Cheng et al., 2013; Zhou et al., 2017), should be larger during this low temperature period. Moreover, levoglucosan~~LG~~/$K^+$ ratios also can be influenced by combustion conditions, i.e., smoldering versus flaming burns. Biofuels are typically subject to smoldering combustion condition in residential stoves for heating purposes in the rural areas in North China, which was reflected in relatively higher levoglucosan~~LG~~/$K^+$ ratios than during flaming combustion (Schkolnik et al., 2005; Lee et al., 2010).

## 4. Summary and conclusion

Anhydrosugars, including levoglucosan and mannosan, and water-soluble potassium ion were employed as molecular tracers to investigate the characteristics of biomass burning activities as well as chemical properties of ambient aerosols under different biomass burning pollution levels. The

measured daily average concentrations of levoglucosan~~LG~~, mannosan~~MN~~ and $K^+$ in $PM_{2.5}$ during a typical biomass burning season from 15 October to 30 November, 2016 were $0.79 \pm 0.75$ μg m$^{-3}$, $0.03 \pm 0.03$ μg m$^{-3}$ and $1.52 \pm 0.62$ μg m$^{-3}$, respectively. The concentrations of carbonaceous components and biomass burning tracers were observed higher at nighttime than daytime, while the patterns of secondary inorganic ions ($SO_4^{2-}$, $NO_3^-$ and $NH_4^+$) were opposite, since they were enhanced by photochemical formation during daytime. An episode with extreme biomass burning tracer levels was encountered on 31 October, 2016, with concentrations of levoglucosan~~LG~~ as high as 4.37 µg m$^{-3}$. Comparing the chemical compositions between different biomass burning periods, it was apparent that biomass burning can considerably elevate the levels of organic components, while not showing a significant effect on the production of secondary inorganic ions. Compared to the other biomass burning episodes, the levoglucosan/mannosan ratios during the heating season period slightly decreased, ~~Moreover, due to more local soft wood and smoldering combustion taking place for heating under the low temperatures, the~~ while levoglucosan~~LG~~/$K^+$ ratio during the intensive BB period was unusually higher than those in the other three biomass burning periods.

***Data availability.*** The data used in this study can be obtained from this open link: https://pan.baidu.com/s/11bKUZff1KJbzNVxS3VsLaA code: jvqx. It is also available from the corresponding author upon request (lianglinlin@cma.gov.cn).

***Author contributions.*** LL designed conducted all observations and drafted the paper. GE revised the paper and improved the English writing. XL drew the Figure 4 and Figure 5. CL, WX, YC, ZD, GZ, JS and XZ interpreted the data and discussed the results. All authors approved the final version for publication.

***Competing interests.*** The authors declare that they have no conflict of interest.

***Special issue statement.*** This article is part of the special issue– "In-depth study of air pollution sources and processes within Beijing and its surrounding region (APHH-Beijing) (ACP/AMT interjournal SI)". It is not associated with a conference.

***Acknowledgements.*** This research is supported by the Beijing Natural Science Foundation (8192055) and CAMS Fundamental Research Funds (No. 2017Z011). The authors would like to

acknowledge Yingli Yu and Ye Kuang for their help with PM$_{2.5}$ samples collection; Hongbing

Cheng for help with chemical analyses.

*Financial support.* This research has been supported by the Beijing Natural Science Foundation

(No. 8192055), State Environmental Protection Key Laboratory of Sources and Control of Air

Pollution Complex (No. SCAPC201701) and Chinese Academy of Meteorological Sciences

Fundamental Research Funds (No. 2017Z011).

**References:**

Bari, M. A., Baumbach, G., Kuch, B., and Scheffknecht, G.: Wood smoke as a source of particle-phase organic compounds in residential areas, Atmos. Environ., 43, 4722-4732, https://doi.org/10.1016/j.atmosenv.2008.09.006, 2009.

Boreddy, S. K. R., Kawamura, K., Okuzawa, K., Kanaya, Y., and Wang, Z.: Temporal and diurnal variations of carbonaceous aerosols and major ions in biomass burning influenced aerosols over Mt. Tai in the North China Plain during MTX2006, Atmos. Environ., 154, 106-117, http://dx.doi.org/10.1016/j.atmosenv.2017.01.042, 2017.

Caseiro, A., Bauer, H., Schmidl, C., Pio, C. A., and Puxbaum, H.: Wood burning impact on PM$_{10}$ in three Austrian regions, Atmos. Environ., 43, 2186-2195, https://doi.org/10.1016/j.atmosenv.2009.01.012, 2009.

Chantara, S., Thepnuan, D., Wiriya, W., Prawan, S., and Tsai, Y.I.: Emissions of pollutant gases, fine particulate matters and their significant tracers from biomass burning in an open-system combustion chamber, Chemos. 224, 407-416, https://doi.org/10.1016/j.chemosphere.2019.02.153, 2019.

Cheng, Y., He, K.B., Du, Z.Y., Engling, G., Liu, J.M., Ma, Y.L., Zheng, M., Weber, R.J.: The characteristics of brown carbon aerosol during winter in Beijing, Atmos. Environ., 127, 355–364, https://doi.org/10.1016/j.atmosenv.2015.12.035, 2016.

Cheng, Y., Engling, G., He, K.B., Duan, F.K., Ma, Y.L., Du, Z.Y., Liu, J.M., Zheng, M., and Weber, R.J.: Biomass burning contribution to Beijing aerosol, Atmos. Chem. Phys., 13, 7765-7781, https://doi.org/10.5194/acp-13-7765-2013, 2013.

Chi, X., He, P., Jiang, Z., Yu, X., Yue, F., Wang, L., Li, B., Kang, H., Liu, C., and Xie, Z.: Acidity of aerosols during winter heavy haze events in Beijing and Gucheng, China, J. Meteorol. Res., 32, 14-25, https://doi.org/10.1007/s13351-018-7063-4, 2018.

Drewnick, F., Hings, S. S., Curtius, J., Eerdekens, G., and Williams, J.: Measurement of fine particulate and gas-phase species during the New Year's fireworks 2005 in Mainz, Germany, Atmos. Environ., 40, 4316-4327, https://doi.org/10.1016/j.atmosenv.2006.03.040, 2006.

Du, Z.Y., He, K.B., Cheng, Y., Duan, F.K., Ma, Y. L., Liu, J.M., Zhang, X.L., Zheng, M., and Weber, R.: A yearlong study of water-soluble organic carbon in Beijing I: Sources and its primary vs. secondary nature, Atmos. Environ., 92, 514-521, https://doi.org/10.1016/j.atmosenv.2014.04.060, 2014.

Duan, F., Liu, X., Yu, T., and Cachier, H.: Identification and estimate of biomass burning contribution to the urban aerosol organic carbon concentrations in Beijing, Atmos. Environ., 38, 1275-1282, https://doi.org/10.1016/j.atmosenv.2003.11.037, 2004.

Engling, G., Carrico, C.M., Kreidenweis, S.M., Collett Jr, J.L., Day, D.E., Malm, W.C., Lincoln, L., Hao, W.M., Iinuma, Y., and Herrmann, H.: Determination of levoglucosan in biomass

combustion aerosol by high-performance anion-exchange chromatography with pulsed amperometric detection, Atmos. Environ., 40, S299-S311, https://doi.org/10.1016/j.atmosenv.2005.12.069, 2006.

Engling, G., Lee, J. J., Tsai, Y. W., Lung, S. C. C., Chou, C. C. K., and Chan, C. Y.: Size resolved anhydrosugar composition in smoke aerosol from controlled field burning of rice straw, Aerosol Sci. Tech., 43, 662-672, https://doi.org/10.1080/02786820902825113, 2009.

Ge, B.Z., Wang, Z.F., Lin, W.L., Xu, X.B., Li, J., Ji, D.S., and Ma, Z.Q.: Air pollution over the north china plain and its implication of regional transport: a new sight from the observed evidences, Environ. Pollut., 166, 29-38, https://doi.org/10.1016/j.envpol.2017.10.084, 2017.

Gensch, I, Sang-Arlt, X,F, Laumer, W, Chan, C,Y, Engling, G, Rudolph, J., and Kiendler-Scharr, A.: Using δ13C of levoglucosan as a chemical clock, Environ. Sci. Tech. https://pubs.acs.org/doi/10.1021/acs.est.8b03054, 2018.

He, K.B., Zhao, Q., Ma, Y.L., Duan, F.K., Yang, F.M., Shi, Z.B., and Chen, G.: Spatial and seasonal variability of PM2.5 acidity at two Chinese megacities: insights into the formation of secondary inorganic aerosols, Atmos. Chem. Phys., 12, 1377-1395, https://doi.org/10.5194/acp-12-1377-2012, 2012.

Hertwig, D., Burgin, L., Gan, C., Hort, M., Jones, A., Shaw, F., Witham, C., and Zhang, K.: Development and demonstration of a Lagrangian dispersion modeling system for real-time prediction of smoke haze pollution from biomass burning in Southeast Asia, J. Geophys. Res.: Atmos., 120, 12605-12630, https://doi.org/10.1002/2015JD023422, 2015.

Ho, K.F., Engling, G., Sai Hang Ho, S., Huang, R., Lai, S., Cao, J., and Lee, S.C.: Seasonal variations of anhydrosugars in PM2.5 in the Pearl River Delta Region, China, Tellus B, 66, 22577, https://doi.org/10.3402/tellusb.v66.22577, 2014.

Jung, J., Lee, S., Kim, H., Kim, D., Lee, H., and Oh, S.: Quantitative determination of the biomass-burning contribution to atmospheric carbonaceous aerosols in Daejeon, Korea, during the rice-harvest period, Atmos. Environ., 89, 642-650, https://doi.org/10.1016/j.atmosenv.2014.03.010, 2014.

Kanakidou, M., Seinfeld, J. H., Pandis, S. N., Barnes, I., Dentener, F. J., Facchini, M. C., Van Dingenen, R., Ervens, B., Nenes, A., Nielsen, C. J., Swietlicki, E., Putaud, J. P., Balkanski, Y., Fuzzi, S., Horth, J., Moortgat, G. K., Winterhalter, R., Myhre, C. E. L., Tsigaridis, K., Vignati, E., Stephanou, E. G., and Wilson, J.: Organic aerosol and global climate modelling: a review, Atmos. Chem. Phys., 5, 1053-1123, https://doi.org/10.5194/acp-5-1053-2005, 2005.

Klejnowski, K., Janoszka, K., and Czaplicka, M.: Characterization and seasonal variations of organic and elemental carbon and levoglucosan in PM$_{10}$ in Krynica Zdroj, Poland, Atmos., 8(10), 190. https://doi.org/10.3390/atmos8100190, 2017.

Kuang, Y., Xu, W.Y., Lin, W.L., Meng, Z.Y., Zhao, H. R., Ren, S.X. Zhang, G., Liang, L. L., and Xu, X. B.: Explosive morning growth phenomena of NH$_3$ on the North China Plain: Causes and potential impacts on aerosol formation, Environ. Pollut., https://doi.org/10.1016/j.envpol.2019.113621, in press, 2020.

Lee, T., Sullivan, A.P., Mack, L., Jimenez, J.L., Kreidenweis, S.M., Onasch, T.B., Worsnop, D.R., Malm, W., Wold, C.E., Hao, W.M., and Collett Jr., J.L.: Chemical smoke marker emissions during flaming and smoldering phases of laboratory open burning of wildland fuels, Aerosol Science and Technology 44. http://dx.doi.org/10.1080/02786826.2010.499884, 2010.

Liang, L., Engling, G., Du, Z., Cheng, Y., Duan, F., Liu, X., and He, K.: Seasonal variations and source estimation of saccharides in atmospheric particulate matter in Beijing, China, Chemosphere, 150, 365-377, 10.1016/j.chemosphere.2016.02.002, 2016.

Liang, L., Engling, G., Zhang, X., Sun, J., Zhang, Y., Xu, W., Liu, C., Zhang, G., Liu, X., and Ma, Q.: Chemical characteristics of PM 2.5 during summer at a background site of the Yangtze River Delta in China, Atmospheric Research, 198, 163-172, 10.1016/j.atmosres.2017.08.012,

493    2017.

494    Liang, L., Engling, G., Cheng, Y., Liu, X., Du, Z., Ma, Q., Zhang, X., Sun, J., Xu, W., Liu, C., Zhang,
495        G., and Xu, H.: Biomass burning impacts on ambient aerosol at a background site in East China:
496        Insights    from    a    yearlong    study,    Atmospheric    Research,    231,    104660,
497        10.1016/j.atmosres.2019.104660, 2020.

498    Lin, W.L., Xu, X.B., Sun, J.Y., Liu, X.W., and Wang, Y.: Background concentrations of reactive
499        gases and the impacts of long-range transport at the jinsha regional atmospheric background
500        station, Science China (Earth Sciences), 54, 1604-1613, 2011.

501    Liu, L., Liu, Y., Wen, W., Liang, L., Ma, X., Jiao, J., and Guo, K.: Source Identification of Trace
502        Elements in PM2.5 at a Rural Site in the North China Plain, Atmos., 11(2),
503        179, https://doi.org/10.3390/atmos11020179, 2020.

504    Meng, Z.Y., Xu, X.B., Lin, W. L., Ge, B.Z., Xie, Y.L., Song, B., Jia, S.H., Zhang, R., Peng, W.,
505        Wang, Y., Cheng, H.B., Yang, W., and Zhao, H.R.: Role of ambient ammonia in particulate
506        ammonium formation at a rural site in the North China Plain, Atmos. Chem. Phys., 18, 167–
507        184, https://doi.org/10.5194/acp-18-167-2018, 2018.

508    Merico, E., Grasso, F.M., Cesari, D., Decesari, S., Belosi, F., Manarini, F.,   De Nuntiis, P., Rinaldi,
509        M., Gambaro, A., Morabito, E., and Contini, D.: Characterisation of atmospheric pollution near
510        an industrial site with a biogas production and combustion plant in southern
511        Italy, https://doi.org/10.1016/j.scitotenv.2020.137220, Sci. Tot. Environ., 717, 137220, 2020.

512    Mkoma, S. L., Kawamura, K., and Fu, P. Q.: Contributions of biomass/biofuel burning to organic
513        aerosols and particulate matter in Tanzania, East Africa, based on analyses of ionic species,
514        organic and elemental carbon, levoglucosan and mannosan, Atmos. Chem. Phys., 13, 10325–
515        10338, https://doi.org/10.5194/acp-13-10325-2013, 2013.

516    Peltier, R. E., Hecobian, A. H., Weber, R. J., Stohl, A., Atlas, E. L., Riemer, D. D., Blake, D. R.,
517        Apel, E., Campos, T., and Karl, T.: Investigating the sources and atmospheric processing of
518        fine particles from Asia and the Northwestern United States measured during INTEX B, Atmos.
519        Chem. Phys., 8, 1835-1853, https://doi.org/10.5194/acp-8-1835-2008, 2008.

520    Pietrograndes, M.C., Bacco, D., Ferrari, S., Kaipainen, J., Ricciardelli, I., Riekkola, M.-L., Trentini,
521        A., and Visentin, M.: Characterization of atmospheric aerosols in the Po valley during the
522        supersito campaigns — Part 3: Contribution of wood combustion to wintertime atmospheric
523        aerosols in Emilia Romagna region (Northern Italy), Atmos. Environ., 122, 291-
524        305, https://doi.org/10.1016/j.atmosenv.2015.09.059, 2015

525    Pope, C.A., and Dockery, D.W.: Health effects of fine particulate air pollution: lines that connect, J.
526        Air Waste Manage., 56, 709-742, https://doi.org/10.1080/10473289.2006.10464485, 2006.

527    Sang, X.F., Zhang, Z.S., Chan, C.Y., and Engling, G.: Source categories and contribution of biomass
528        smoke to organic aerosol over the southeastern Tibetan plateau, Atmos. Environ., 78, 113-
529        123, https://doi.org/10.1016/j.atmosenv.2012.12.012, 2013.

530    Sang, X.F., Gensch, I., Kammer, B., Khan, A., Kleist, E., Laumer, W., Schlag, P., Schmitt, S.H.,
531        Wildt, J., Zhao, R., Mungall, E.L., Abbatt, J.P.D., and Kiendler-Scharr, A.: Chemical stability
532        of    levoglucosan:    An    isotopic    perspective,    J.    Geophys.    Res.,    43,    5419-
533        5424, https://doi.org/10.1002/2016GL069179, 2016.

534    Schkolnik, G., Falkovich, A.H., Rudich, Y., Maenhaut, W., and Artaxo, P.: New analytical method
535        for the determination of levoglucosan, polyhydroxy compounds, and 2-methylerythritol and its
536        application    to    smoke    and    rainwater    samples,    Environ.    Sci.    Technol.,    39,    2744-
537        2752, https://doi.org/10.1021/es048363c, 2005.

538    Shen, X.J., Sun, J.Y., Zhang, X.Y., Zhang, Y.M., Wang, Y.Q., Tan, K.Y., Wang, P., Zhang, L., Qi,
539        X.F., Che, H.Z., Zhang, Z., Zhong, J.T., Zhao, H.R., and Ren, S.X.: Comparison of submicron
540        particles at a rural and an urban site in the North China Plain during the December 2016 heavy
541        pollution episodes, J. Meteorol. Res., 32, 14-25, https://doi.org/10.1007/s13351-018-7060-7,

542    2018.

543    Streets, D.G., Bond, T.C., Carmichael, G.R., Fernandes, S.D., Fu, Q., He, D., Klimont, Z., Nelson,
544        S.M., Tsai, N.Y., Wang, M.Q., Woo, J.H., and Yarber, K.F.: An inventory of gaseous and
545        primary aerosol emissions in Asia in the year 2000, J. Geophys. Res., 108 (D21),
546        8809. http://dx.doi.org/10.1029/2002JD003093, 2003.

547    Sullivan, A.P., Holden, A.S., Patterson, L.A., McMeeking, G.R., Kreidenweis, S.M., Malm, W.C.,
548        Hao, W.M., Wold, C.E., and Collett Jr., J.L.: A method for smoke marker measurements and
549        its potential application for determining the contribution of biomass burning from wildfires
550        and prescribed fires to ambient $PM_{2.5}$ organic carbon, J. Geophys. Res., 113,
551        D22302, https://doi.org/10.1029/2008JD010216, 2008.

552    Sun, K., Liu, X.G., Gu, J.W., Li, Y.P., Qu, Y., An, J.L., Wang, J.L., Zhang, Y.H., Hu, M., Zhang, F.:
553        Chemical characterization of size-resolved aerosols in four seasons and hazy days in the
554        megacity    Beijing    of    China,    J.    Environ.    Sci.,    32,    155-
555        167, https://doi.org/10.1016/j.jes.2014.12.020, 2015.

556    Sun, Y.L., Wang, Z.F., Fu, P.Q., Yang, T., Jiang, Q., Dong, H.B., Li, J., and Jia, J.J.: Aerosol
557        composition, sources and processes during wintertime in Beijing, China, Atmos. Chem. Phys.,
558        13, 4577-4592, https://doi.org/10.5194/acp-13-4577-2013, 2013.

559    Sun, Y.L., Zhang, Q., Anastasio, C., and Sun, J.: Insights into secondary organic aerosol formed via
560        aqueous-phase reactions of phenolic compounds based on high resolution mass spectrometry,
561        Atmos. Chem. Phys., 10, 4809-4822, https://doi.org/10.5194/acp-10-4809-2010, 2010.

562    Tan, J.H., Duan, J.C., Zhen, N.J., He, K.B., and Hao, J.M.: Chemical characteristics and source of
563        size-fractionated atmospheric particle in haze episode in Beijing, Atmos. Res., 167, 24-
564        33, https://doi.org/10.1016/j.atmosres.2015.06.015, 2016.

565    Tang, R., Wu, Z., Li, X., Wang, Y., Shang, D., Xiao, Y., Li, M., Zeng, L., Wu, Z., Hallquist, M., Hu,
566        M., and Guo, S.: Primary and secondary organic aerosols in summer 2016 in Beijing, Atmos.
567        Chem. Phys., 18, 4055-4068, https://doi.org/10.5194/acp-18-4055-2018, 2018.

568    Urban, R.C., Lima-Souza, M., Caetano-Silva, L., Queiroz, M.E.C., Nogueira, R.F.P., Allen, A.G.,
569        Cardoso, A.A., Held, G., and Campos, M.L. A.M.: Use of levoglucosan, potassium, and water-
570        soluble organic carbon to characterize the origins of biomass-burning aerosols, Atmos.
571        Environ., 61, 562-569, https://doi.org/10.1016/j.atmosenv.2012.07.082, 2012.

572    Wang, Z., Wang, T., Guo, J., Gao, R., Xue, L.K., Zhang, J.M., Zhou, Y., Zhou, X.H., Zhang, Q.Z.,
573        and Wang, W.X., 2012. Formation of secondary organic carbon and cloud impact on
574        carbonaceous aerosols at Mount Tai, North China, Atmos, Environ., 46, 516-
575        527, https://doi.org/10.1016/j.atmosenv.2011.08.019, 2012.

576    Wu, Y., Ge, X., Wang, J., Shen, Y., Ye, Z., Ge, S., Wu, Y., Yu, H., and Chen, M.: Responses of
577        secondary aerosols to relative humidity and photochemical activities in an industrialized
578        environment    during    late    winter,    Atmospheric    Environment,    193,    66-78,
579        10.1016/j.atmosenv.2018.09.008, 2018.

580    Xu, W., Kuang, Y., Zhao, C., Tao, J., Zhao, G., Bian, Y., Yang, W., Yu, Y., Shen, C., Liang, L., Zhang,
581        G., Lin, W., and Xu, X.: $NH_3$-promoted hydrolysis of $NO_2$ induces explosive growth in HONO,
582        Atmos. Chem. Phys., 19, 10557-10570, https://doi.org/10.5194/acp-19-10557-2019, 2019

583    Xu, W., Kuang, Y., Liang, L., He, Y., Cheng, H., Bian, Y., Tao, J., Zhang, G., Zhao, P., Ma, N., Zhao,
584        H., Zhou, G., Su, H., Cheng, Y., Xu, X., Shao, M., and Sun, Y.: Dust-Dominated Coarse
585        Particles as a Medium for Rapid Secondary Organic and Inorganic Aerosol Formation in
586        Highly Polluted Air, Environ Sci Technol, 54, 15710-15721, 10.1021/acs.est.0c07243, 2020.

587    Xu, X., Zhang, H., Lin, W., Wang, Y., Xu, W., and Jia, S.: First simultaneous measurements of
588        peroxyacetyl nitrate (PAN) and ozone at Nam Co in the central Tibetan Plateau: impacts from
589        the PBL evolution and transport processes, Atmos. Chem. Phys., 18, 5199–
590        5217, https://doi.org/10.5194/acp-18-5199-2018, 2018.

Yang, F.M., Tan, J.H., Zhao, Q. Du, Z.Y., He, K.B., Ma, Y.L., Duan, F.K., Chen, G., and Zhao, Q.: Characteristics of $PM_{2.5}$ speciation in representative megacities and across China, Atmos. Chem. Phys., 11, 5207-5219, https://doi.org/10.5194/acp-11-5207-2011, 2011.

Yao, L., Yang, L.X., Chen, J.M., Wang, X.F., Xue, L.K., Li, W.J., Sui, X., Wen, L., Chi, J.W., Zhu, Y.H., Zhang, J.M., Xu, C.H., Zhu, T., and Wang, W.X.: Characteristics of carbonaceous aerosols: Impact of biomass burning and secondary formation in summertime in a rural area of the North China Plain, Sci. Tot. Environ., 557-558, https://doi.org/10.1016/j.scitotenv.2016.03.111, 2016.

Yu, J.T., Yan, C.Q., Liu, Y., Li, X.Y., Zhou, T., and Zheng, M.: Potassium: A Tracer for Biomass Burning in Beijing? Aerosol Air Qual. Res., 18, 2447-2459, doi: 10.4209/aaqr.2017.11.0536, 2018.

Zhang, T., Cao, J.J., Chow, J.C., Shen, Z.X., Ho, K.F., Ho, S.S.H., Liu, S.X., Han, Y.M., Watson, J.G., Wang, G.H., and Huang, R.J.: Characterization and seasonal variations of levoglucosan in fine particulate matter in Xi'an, China, J. Air Waste Manage., 64, 1317-1327, https://doi.org/10.1080/10962247.2014.944959, 2014.

Zhang, T., Claeys, M., Cachier, H., Dong, S.P., Wang, W., Maenhaut, W., and Liu, X.D.: Identification and estimation of the biomass burning contribution to Beijing aerosol using levoglucosan as a molecular marker, Atmos. Environ., 42, 7013-7021, https://doi.org/10.1016/j.atmosenv.2008.04.050, 2008.

Zhang, Z., Engling, G., Lin, C.-Y., Chou, C. C. K., Lung, S.-C. C., Chang, S.-Y., Fan, S., Chan, C.-Y., and Zhang, Y.-H.: Chemical speciation, transport and contribution of biomass burning smoke to ambient aerosol in Guangzhou, a mega city of China, Atmospheric Environment, 44, 3187-3195, 10.1016/j.atmosenv.2010.05.024, 2010.

Zhang, Z., Gao, J., Engling, G., Tao, J., Chai, F., Zhang, L., Zhang, R., Sang, X., Chan, C.Y., Lin, Z., and Cao, J.: Characteristics and applications of size-segregated biomass burning tracers in China's Pearl River Delta region, Atmos. Environ., 102, 290-301, https://doi.org/10.1016/j.atmosenv.2014.12.009, 2015.

Zheng, G.J., Duan, F.K., Su, H., Ma, Y.L., Cheng, Y., Zheng, B., Zhang, Q., Huang, T., Kimoto, T., Chang, D., Pöschl, U., Cheng, Y. F., and He, K. B.: Exploring the severe winter haze in Beijing: the impact of synoptic weather, regional transport and heterogeneous reactions, Atmos. Chem. Phys., 15, 2969-2983, https://doi.org/10.5194/acp-15-2969-2015, 2015.

Zheng, M., Salmon, L. G., Schauer, J. J., Zeng, L., Kiang, C. S., Zhang, Y., and Cass, G. R.: Seasonal trends in $PM_{2.5}$ source contributions in Beijing, China, Atmos. Environ., 39, 3967-3976, https://doi.org/10.1016/j.atmosenv.2005.03.036, 2005.

Zhong, J.T., Zhang, X.Y., and Wang, Y.Q.: Reflections on the threshold for $PM_{2.5}$ explosive growth in the cumulative stage of winter heavy aerosol pollution episodes (HPEs) in Beijing, Tellus B, 71, 1-7, https://doi.org/10.1080/16000889.2018.1528134, 2019.

Zhong, J.T., Zhang, X.Y., Wang, Y.Q., Liu, C., and Dong, Y.S.: Heavy aerosol pollution episodes in winter Beijing enhanced by radiative cooling effects of aerosols, Atmos. Res., 209, 59-64, https://doi.org/10.1016/j.atmosres.2018.03.011, 2018.

Zhou, Y., Xing, X., Lang, J., Chen, D., Cheng, S., Wei, L., Wei, X., and Liu, C.: A comprehensive biomass burning emission inventory with high spatial and temporal resolution in China, Atmos. Chem. Phys., 17, 2839-2864, 10.5194/acp-17-2839-2017, 2017.

Zhu, C., Kawamura, K., and Kunwar, B.: Effect of biomass burning over the western North Pacific Rim: wintertime maxima of anhydrosugars in ambient aerosols from Okinawa, Atmos. Chem. Phys., 15, 1959-1973, https://doi.org/10.5194/acp-15-1959-2015, 2015.

Zhu, Y.H., Yang, L.X., Kawamura, K., Chen, J.M., Ono, K., Wang, X.F., Xue, L.K., and Wang, W.X.: Contributions and source identification of biogenic and anthropogenic hydrocarbons to secondary organic aerosols at Mt. Tai in 2014, Environ. Pollut., 220, 863-

640 872, https://doi.org/10.1016/j.envpol.2016.10.070, 2017.

641

642

643

644

645

646

647

648

649

650

651

652

653

654

655

656

657

658 **Table 1.** Average concentrations and the range of $PM_{2.5-ca1}$ and its chemical components, biomass burning

659 tracers (µg m$^{-3}$), gaseous species, ratios of OC/EC and levoglucosan LG/OC, as well as meteorological

660 data observed at GC site at daytime, nighttime and whole day, respectively, during the sampling period

661 from 15 Oct to 23 Nov 2016.

| Species | Daytime (N = 34) | | Nighttime (N = 33) | | Whole period (N = 37)* | |
| --- | --- | --- | --- | --- | --- | --- |
| | Average cConcentration | Range | Average concentrationConcentration | Range | Average concentrationConcentration | Range |
| $PM_{2.5-cal}$ | $117 \pm 58.8$ | 19.0 - 225 | $170 \pm 116$ | 21.1 - 465 | $137 \pm 72.4$ | 23.3 - 319 |
| OC | $26.8 \pm 15.7$ | 3.78 - 64.8 | $61.6 \pm 49.5$ | 2.88 - 175 | $44.0 \pm 31.0$ | 4.13 - 117 |
| EC | $13.4 \pm 8.49$ | 1.44 - 34.0 | $30.9 \pm 28.5$ | 2.21 - 129 | $21.7 \pm 15.8$ | 2.46 - 74.9 |
| TC | $49.3 \pm 27.6$ | 5.76 - 124 | $92.5 \pm 73.6$ | 5.10 - 289 | $65.8 \pm 44.1$ | 7.36 - 192 |
| OC/EC | $2.02 \pm 1.26$ | 1.09 - 3.31 | $2.25 \pm 1.04$ | 1.04 - 6.72 | $1.95 \pm 0.60$ | 0.83 - 3.10 |
| $SO_4^{2-}$ | $12.1 \pm 9.31$ | 1.65 - 39.7 | $9.02 \pm 6.22$ | 1.55 - 23.2 | $10.5 \pm 6.87$ | 1.66 - 29.5 |
| $NO_3^-$ | $16.9 \pm 9.96$ | 1.85 - 41.2 | $13.1 \pm 8.52$ | 1.56 - 38.0 | $15.9 \pm 9.29$ | 2.40 - 45.2 |
| $Cl^-$ | $4.33 \pm 2.30$ | 0.82 - 9.46 | $6.08 \pm 4.00$ | 0.62 – 16.0 | $4.90 \pm 2.46$ | 0.93 - 9.37 |
| $NH_4^+$ | $11.7 \pm 6.76$ | 1.84 - 26.0 | $10.0 \pm 5.75$ | 1.33 - 22.2 | $10.9 \pm 5.51$ | 1.99 - 25.4 |
| $K^+$ | $1.43 \pm 0.54$ | 0.20 - 2.64 | $1.78 \pm 0.95$ | 0.22 - 4.19 | $1.52 \pm 0.62$ | 0.50 - 2.96 |
| $Mg^{2+}$ | $0.26 \pm 0.14$ | 0.07-0.64 | $0.19 \pm 0.09$ | 0.06 - 0.38 | $0.14 \pm 0.12$ | 0.04 - 0.43 |
| $Ca^{2+}$ | $2.24 \pm 1.01$ | 1.02-4.75 | $1.56 \pm 0.08$ | 0.77 - 3.56 | $1.54 \pm 0.90$ | 0.49 - 3.84 |

| Species | | | | | | |
|---|---|---|---|---|---|---|
| $Na^+$ | 0.44 ± 0.17 | 0.10 - 0.79 | 0.43 ± 0.24 | 0.10 - 1.31 | 0.42 ± 0.17 | 0.11 - 0.88 |
| $NO_3^-$ / $SO_4^{2-}$ | 1.67 ± 0.82 | 0.75 - 5.52 | 1.54 ± 0.57 | 0.74 - 3.50 | 1.65 ± 0.62 | 0.78 ± 3.96 |
| Levoglucosan | 0.57 ± 0.62 | 0.05 - 3.74 | 1.10 ± 0.99 | 0.05 - 4.82 | 0.79 ± 0.75 | 0.14 - 4.37 |
| Mannosan | 0.024 ± 0.023 | 0.00 - 0.14 | 0.05 ± 0.04 | 0.00 - 0.21 | 0.03 ± 0.03 | 0.00 - 0.18 |
| levoglucosan~~LG~~/OC | 0.018 ± 0.011 | 0.005 - 0.067 | 0.020 ± 0.010 | 0.004 - 0.047 | 0.020 ± 0.009 | 0.006 - 0.045 |
| NO (ppb) | 23.0 ± 14.7 | 2.07 - 56.0 | 45.9 ± 29.5 | 1.59 - 96.9 | 31.8 ± 18.3 | 1.81 - 68.5 |
| $NO_2$ (ppb) | 25.8 ± 10.4 | 8.18 - 51.6 | 29.3 ± 9.37 | 8.81 - 51.1 | 26.6 ± 8.74 | 8.62 - 51.4 |
| $SO_2$ (ppb) | 9.78 ± 4.96 | 3.11 - 22.5 | 9.63 ± 5.67 | 2.91 - 28.7 | 8.61 ± 4.04 | 3.37 - 20.4 |
| CO (ppm) | 0.96 ± 0.73 | 0.03 - 2.49 | 1.29 ± 1.04 | 0.02 - 3.26 | 1.05 ± 0.76 | 0.12 - 2.48 |
| $O_3$ (ppb) | 13.0 ± 9.10 | 1.42 - 41.84 | 5.00 ± 5.73 | 1.60 - 24.30 | 9.25 ± 5.78 | 1.67 - 24.0 |
| $NH_3$ (ppb) | 16.4 ± 11.3 | 1.68 - 46.2 | 18.3 ± 10.7 | 1.03 - 42.7 | 17.1 ± 9.88 | 1.46 - 44.4 |
| Temperature (°C) | 7.71 ± 4.01 | - 2.07-15.9 | 3.30 ± 4.69 | - 6.60 - 14.5 | 6.95 ± 4.58 | - 4.33 - 15.4 |
| Relative Humidity (%) | 68 ± 17 | 31 - 98 | 85 ± 14 | 34 - 100 | 77 ± 13 | 48 - 99 |
| Wind speed (m s$^{-1}$) | 1.43 ± 1.17 | 0.09 - 5.65 | 0.79 ± 1.55 | 0.03 - 7.19 | 1.07 ± 1.14 | 0.04 - 5.02 |

662     * Six whole-day samples were included ~~used~~ in the data analysis of the "Whole period".

663

664

665

666

667

668

669 **Table 2.** Concentrations of chemical components in $PM_{2.5}$ aerosols as well as their ratios and gaseous

670 species collected at the GC site, during the four biomass burning periods (i.e., Minor, Intensive, Major

671 and Heating period) from 15 Oct to 23 Nov 2016.

| Species | Period I (15-30 Oct) Minor BB | | Period II (31 Oct) Intensive BB | | Period III (1 -14, Nov) Major BB | | Period IV (15 -23, Nov) Heating period | |
|---|---|---|---|---|---|---|---|---|
| | Average ~~C~~concentration | | Average concentration~~C oncentration~~ | Ratio* | Average concentration ~~Concentration~~ | Ratio* | Average concentration~~Co ncentration~~ | Ratio* |
| $PM_{2.5-cal}$ | 81.0 ± 44.5 | | 235 | 2.91 | 163 ± 46.7 | 2.01 | 189 ± 83.0 | 2.33 |
| Levoglucosan | 0.36 ± 0.14 | | 4.37 | 12.1 | 0.90 ± 0.37 | 2.50 | 0.96 ± 0.63 | 2.67 |
| Mannosan | 0.015 ± 0.005 | | 0.18 | 12.0 | 0.038 ± 0.015 | 2.53 | 0.050 ± 0.026 | 3.33 |
| OC | 16.2 ± 7.52 | | 96.3 | 5.93 | 55.2 ± 17.1 | 3.41 | 69.4 ± 24.6 | 4.28 |
| EC | 12.2 ± 5.85 | | 36.0 | 2.96 | 25.5 ± 10.1 | 2.09 | 36.4 ± 21.5 | 2.98 |
| TC | 28.4 ± 13.1 | | 132 | 4.66 | 80.9 ± 34.6 | 2.85 | 106 ± 55.3 | 3.73 |
| $SO_4^{2-}$ | 10.3 ± 8.96 | | 4.56 | 0.44 | 11.8 ± 6.02 | 1.15 | 9.08 ± 3.87 | 0.88 |
| $NO_3^-$ | 16.6 ± 12.9 | | 18.1 | 1.09 | 16.5 ± 6.42 | 0.99 | 12.6 ± 5.76 | 0.76 |
| $NH_4^+$ | 10.1 ± 7.40 | | 10.0 | 0.99 | 12.0 ± 4.35 | 1.19 | 10.3 ± 3.62 | 1.02 |
| $K^+$ | 1.16 ± 0.36 | | 2.61 | 2.25 | 1.76 ± 0.46 | 1.52 | 1.65 ± 0.84 | 1.42 |
| $Cl^-$ | 3.46 ± 1.97 | | 7.49 | 2.16 | 5.58 ± 2.16 | 1.61 | 6.27 ± 2.58 | 1.81 |
| OC/EC | 1.53 ± 0.35 | | 2.67 | 1.75 | 2.31 ± 0.59 | 1.51 | 2.04 ± 0.31 | 1.33 |
| $NO_3^-/SO_4^{2-}$ | 1.74 ± 0.60 | | 3.96 | 2.28 | 1.50 ± 0.35 | 0.86 | 1.42 ± 0.47 | 0.82 |

| | | | | | | | |
|---|---|---|---|---|---|---|---|
| levoglucosan-~~LG~~/OC | 0.025 ± 0.008 | 0.045 | 1.80 | 0.016 ± 0.005 | 0.64 | 0.014 ± 0.006 | 0.56 |
| levoglucosan ~~LG~~/EC | 0.039 ± 0.019 | 0.121 | 3.10 | 0.038 ± 0.017 | 0.97 | 0.028 ± 0.013 | 0.72 |
| levoglucosan-~~LG~~/ mannosan~~MN~~ | 24.9 ± 4.44 | 24.1 | 0.97 | 24.8 ± 6.46 | 1.00 | 18.3 ± 4.27 | 0.73 |
| levoglucosan~~L G~~/K$^+$ | 0.36 ± 0.081 | 1.67 | 4.64 | 0.51 ± 0.16 | 1.42 | 0.53 ± 0.15 | 1.47 |
| NO (ppb) | 21.7 ± 12.5 | 21.7 | 1.00 | 39.6 ± 15.4 | 1.82 | 39.3 ± 23.6 | 1.81 |
| NO$_2$ (ppb) | 21.8 ± 4.95 | 26.5 | 1.22 | 32.7 ± 7.27 | 1.50 | 24.6 ± 10.2 | 1.13 |
| NO$_X$ (ppb) | 43.6 ± 16.3 | 48.2 | 1.11 | 72.4 ± 17.8 | 1.66 | 64.0 ± 33.4 | 1.47 |
| SO$_2$ (ppb) | 5.83 ± 2.46 | 8.04 | 1.38 | 11.1 ± 4.10 | 1.90 | 9.75 ± 3.31 | 1.67 |
| CO (ppm) | 0.44 ± 0.33 | 0.70 | 1.59 | 1.65 ± 0.53 | 3.75 | 1.18 ± 0.83 | 2.68 |
| O$_3$ (ppb) | 9.79 ± 4.88 | 23.2 | 2.37 | 7.51 ± 3.87 | 0.77 | 9.59 ± 7.55 | 0.98 |
| NH$_3$ (ppb) | 14.3 ± 6.12 | 11.1 | 0.78 | 18.6 ± 8.03 | 1.30 | 21.2 ± 14.2 | 1.48 |

672     *: indicates that the ratios of the heating period, intense BB period or major biomass burning period

673     were divided by those from the minor BB period.

674

675

676

677

678

679

680
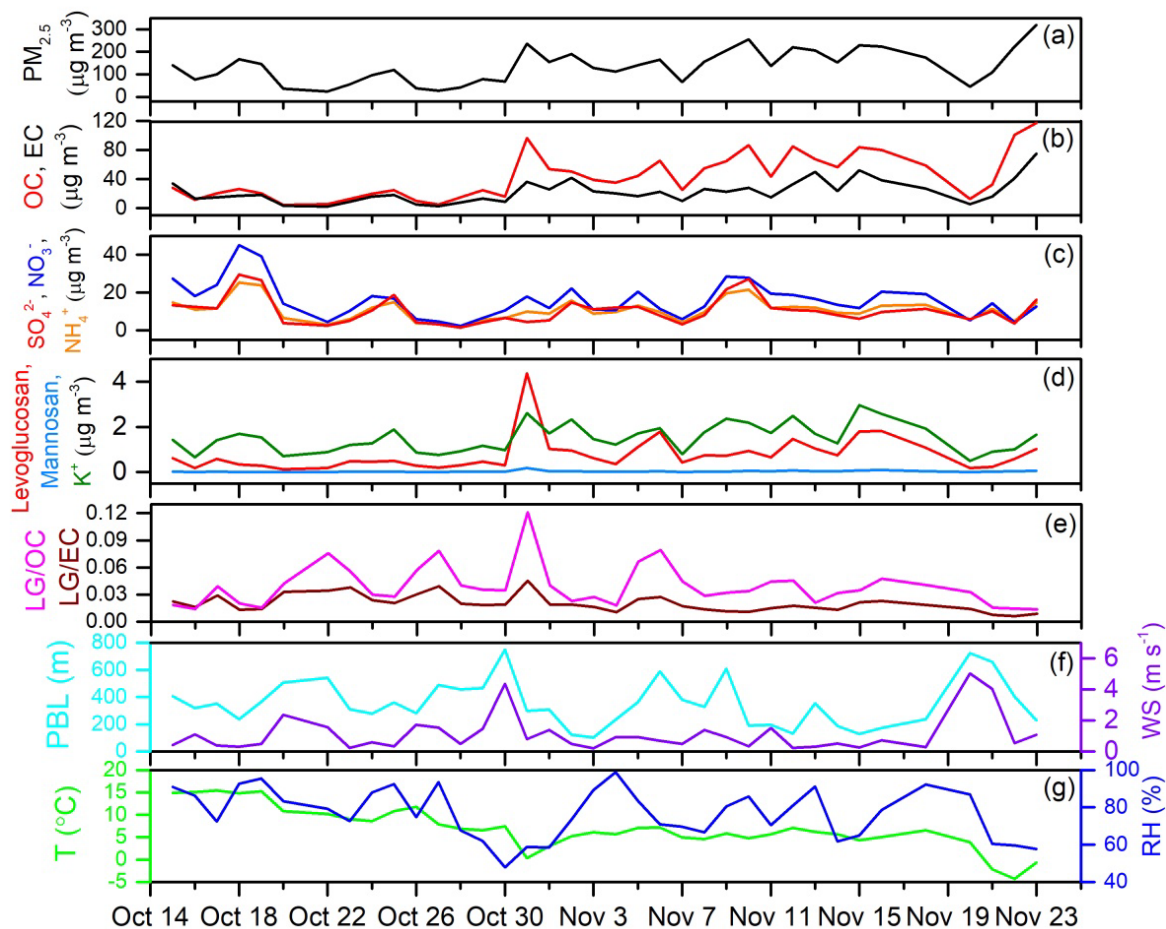
682    **Figure 1.** Time-series variation obtained for PM$_{2.5\text{-cal}}$ and its major components, biomass burning tracers

683    as well as meteorological factors at the GC site during the sampling period from 15 Oct to 23 Nov 2016.

684    (a) PM$_{2.5\text{-cal}}$, and its major components (b) OC, and EC, (c) secondary inorganic aerosols, i.e., SO$_4^{2-}$,

685    NO$_3^-$ and NH$_4^+$, (d) biomass burning tracers (levoglucosanLG, mannosanMN and K$^+$), (e) ratios of

686    levoglucosan to OC (LG/OC) and levoglucosan to EC (LG/EC), and meteorological factors (f) PBL and

687    wind speed (WS), (g) temperature (T) and, relative humidity (RH), wind speed (WS) and rainfall) at the

688    GC site during the sampling period from 15 Oct to 23 Nov 2016.

689

690

691

692

693

694

695

696

697

698

699

700
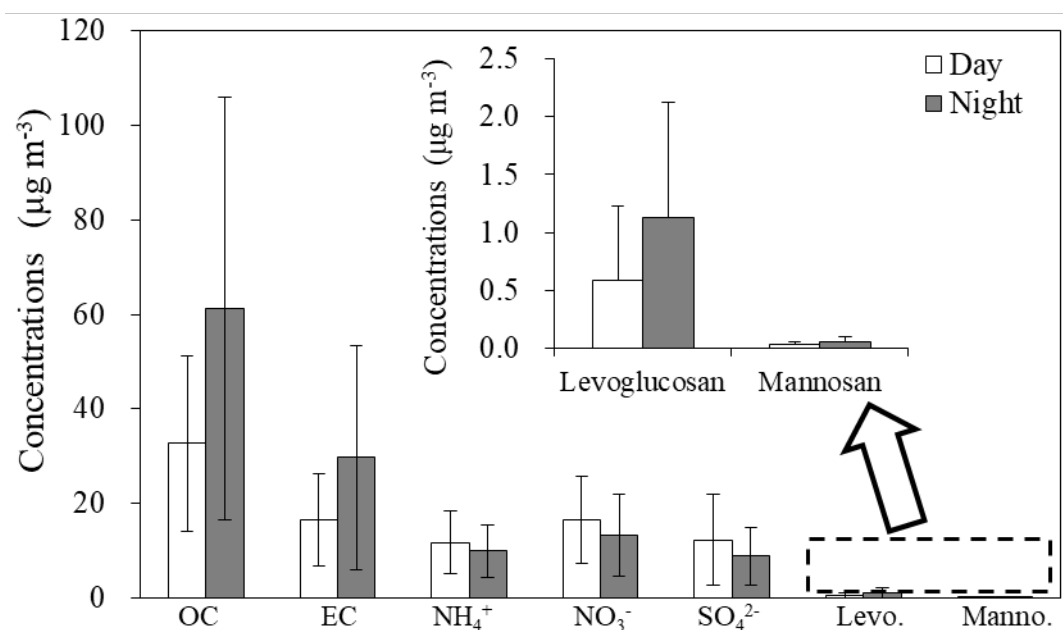
**Figure 2.** Day and night distributions of mean concentrations of main chemical components (OC, EC, $SO_4^{2-}$, $NO_3^-$ and $NH_4^+$) and biomass burning tracers (levoglucosan LG and mannosanMN) in $PM_{2.5}$ observed at GC site during the sampling period.

704

705

706

707

708

709

710

711

712

713

714

715

716

717

718

719

720

721

722
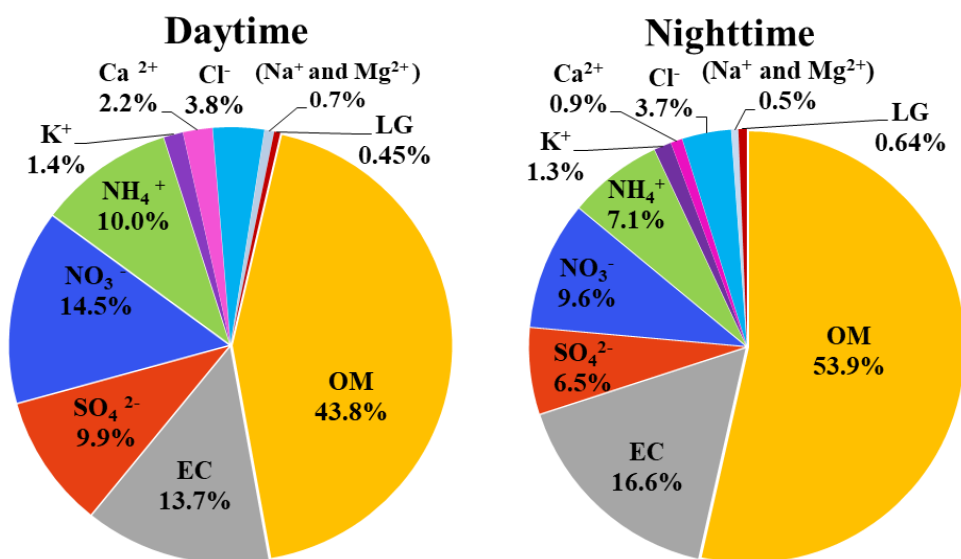
**Figure 3.** Percent contributions of individual component mass concentrations to total estimated PM$_{2.5\text{-cal}}$

mass in daytime and nighttime during the sampling period.

725

726

727

728

729

730

731

732

733
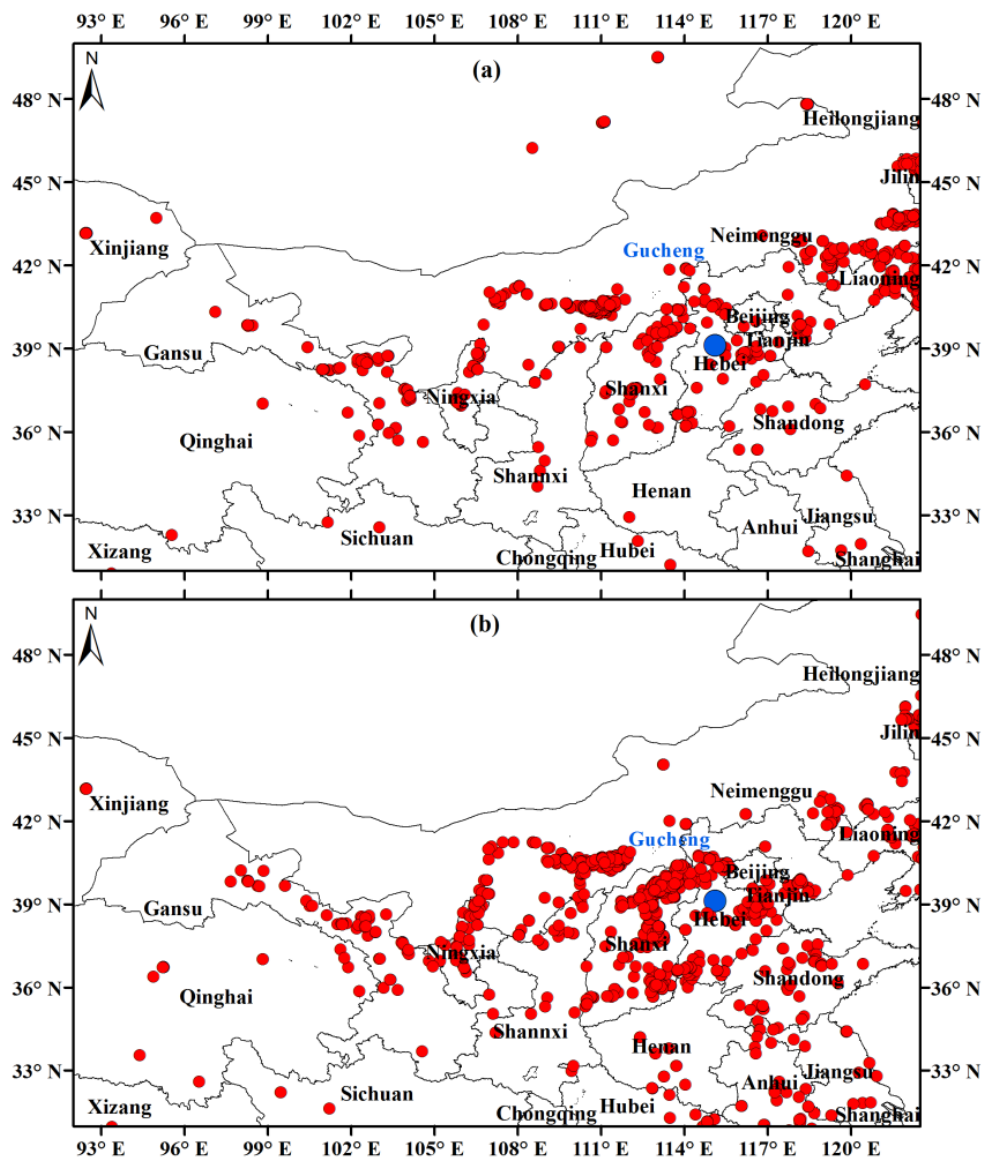
**Figure 4.** Fire spots at GC site and the surrounding provinces from (a) 15-30 October, 2016 and (b) 1 -

23, November, 2016, observed by MODIS Terra satellites (blue dot is GC station).

736

737

738

739

740
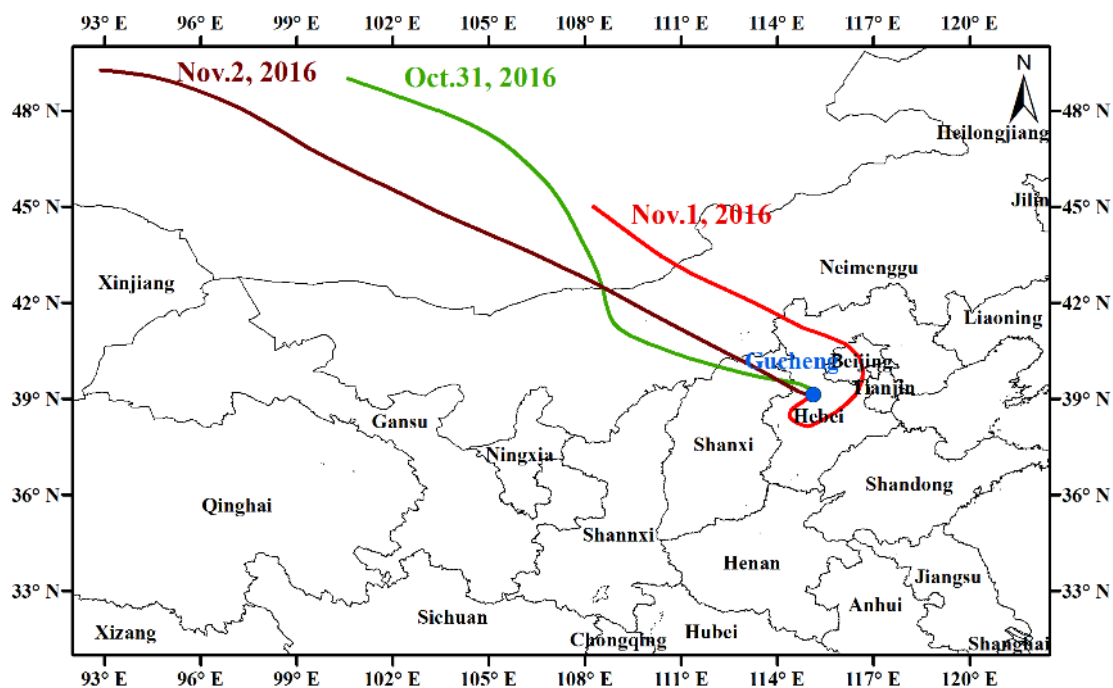
741 **Figure 5.** 48 h back trajectories at 500 m at GC site (39°09'N, 115°44'E) at 00:00 (UTC time) from 31

742 October to 2 November, 2016.

743

744

745

746

747

748

749

750

751

752

753

754

755
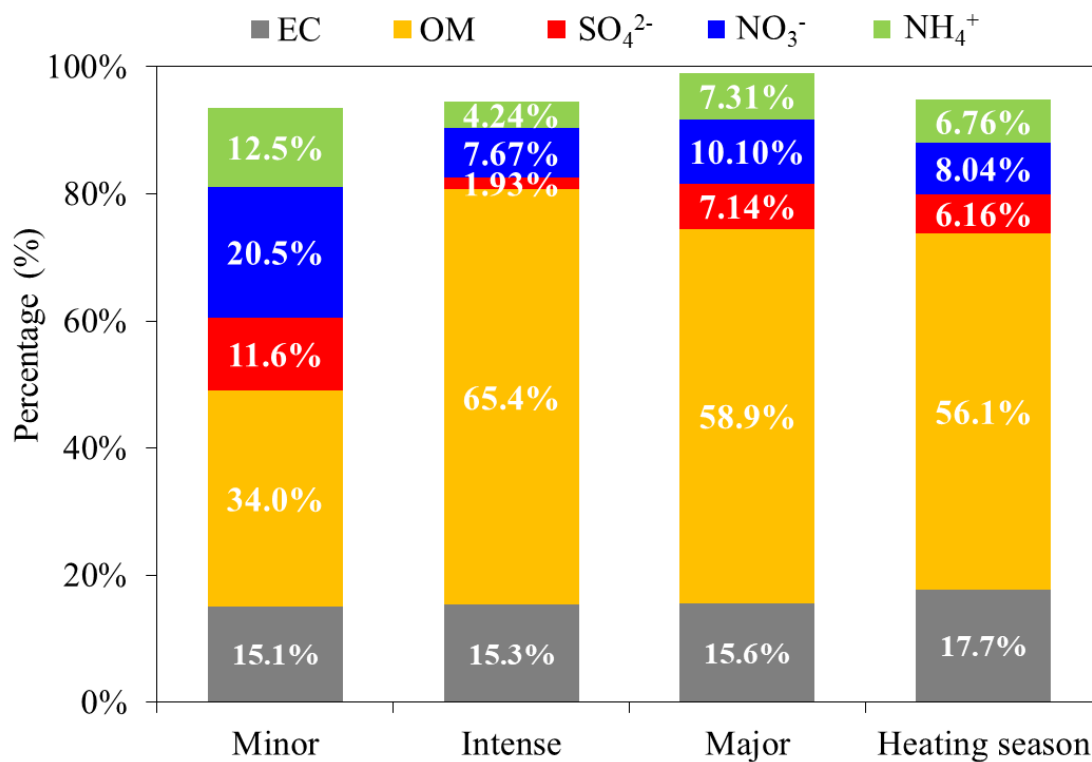
**Figure 6.** Mean percentiles of major components in $PM_{2.5}$ with respect to different biomass burning

pollution periods at GC site during the sampling time.

758

759

760

761

762

763

764

765

766

767

768

769

770

771

772

773

774

775
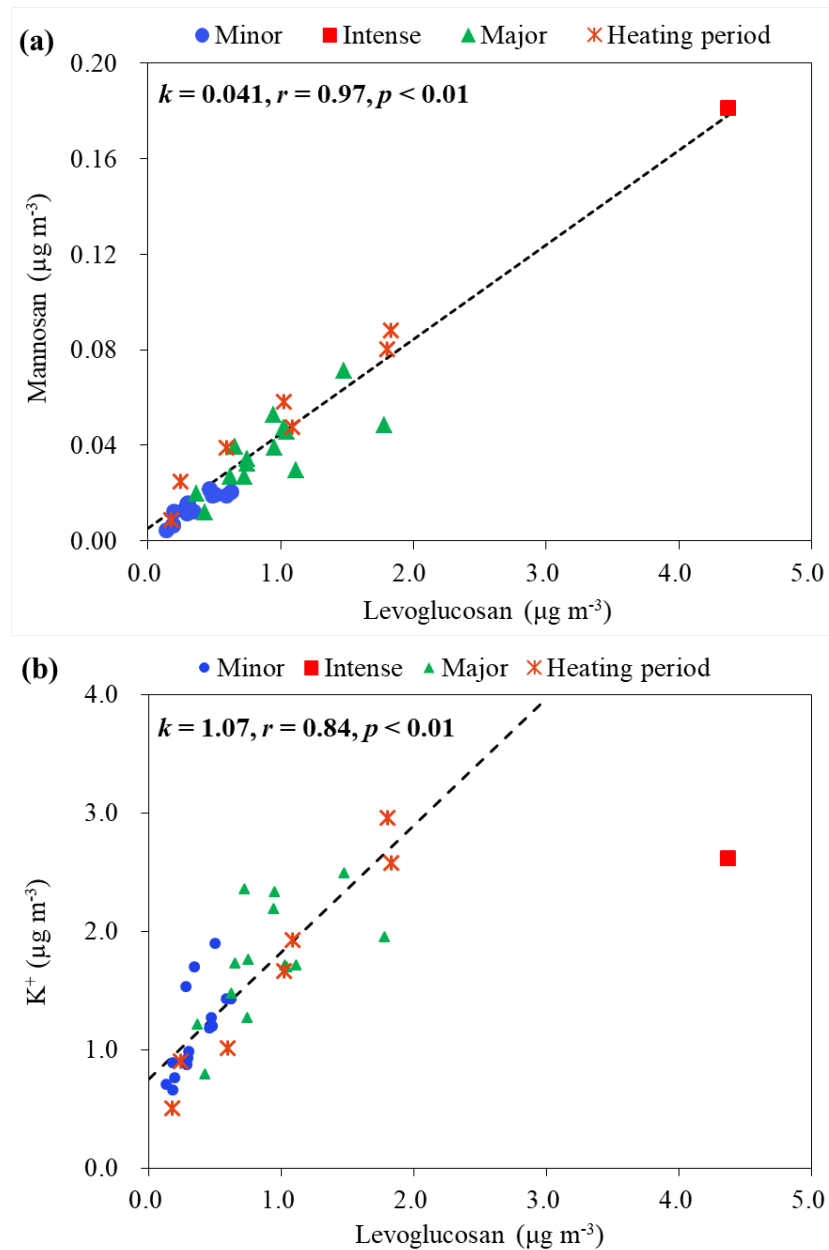
**Figure 7.** Scatter plots of (a) levoglucosan versus mannosan, (b) levoglucosan versus K⁺. Statistical

analysis of sampling data was conducted with the linear fitting method.

778

779

780

781

782

783

784